JOURNAL OF MATERIALS SCIENCE **40** (2005) 1923– 1928

Rate-dependent indentation behavior of solder alloys

FENG-JIANG WANG*,‡
State Key Laboratory of Advanced Welding Production Technology, Harbin Institute of Technology, Harbin 150001, People's Republic of China
E-mail: wangfj@hit.edu.cn

XIN MA
Yik Shing Tat Industrial Co., Ltd., Shenzhen 518101, People's Republic of China

YI-YU QIAN
State Key Laboratory of Advanced Welding Production Technology, Harbin Institute of Technology, Harbin 150001, People's Republic of China

Finite element (FE) simulations of visco-plastic indentation in Sn-37Pb eutectic solder alloy are performed to investigate the influence of loading rate on its creep characteristic. The resulting indentation load-displacement curves are rate-dependent and have varying creep penetration depths during the same hold time. Creep indentation hardness H, defined from the concept of "work of indentation", varies with volume strain occurring during the creep hold time, which is a measure of creep strain rate $\dot{\varepsilon}_{cr}$. Thus, creep stress sensitivity can be determined from the H versus $\dot{\varepsilon}_{cr}$ curve. This analysis can be verified by the good agreement between the derived value and the predefined value, and then be used to analyze the Berkovich indentation load-displacement curves of Sn-3.5Ag-0.75Cu lead-free solder. Such indentation tests and physical analysis provide a cheaper and more convenient method to determine the mechanical properties of the upcoming lead-free solder alloys.

1. Introduction

Lead-free solder alloys have been greatly concerned in recent years due to the increasing requirement for the environmental-friendly electronic packaging and assembly, i.e., prohibition of using certain toxic substances, such as lead. Numerous Sn-based Pb-free alloys have been developed to replace the traditional Sn-Pb solders [1–3]. Obviously, the new Pb-free solder should not only have a chemical composition without lead, but also provide suitable properties to satisfy the requirement of soldering application. Therefore, the evaluation of the mechanical property of Pb-free solder is necessary since it is essential to the long-term reliability of solder joint. Although the conventional tensile test is effective for such purpose, it will cost too much money and time since there are so many candidates as Pb-free solders. Naturally, a cheaper and more convenient experimental method is expected.

Depth-sensing indentation test, as reviewed by Fujiwara *et al*. [4], which is a convenient, non-destructive and low-cost test method, could be a reasonable solution for the above expectation. For rate-independent materials, numerous works have been performed to determine the elastic modulus and yield stress from the indentation load-displacement curves [5–9]. While, for solder alloy that has a high homologous temperature, it is well known that its mechanical properties are significantly rate-dependent and creep damage plays an important role on the long-term reliability of solder joint [10, 11]. Therefore, to directly derive the creep properties, e.g., rate sensitivity, from the indentation load-displacement curves is a key point for the application of depth-sensing indentation test on the mechanical evaluation of solder alloys.

In this work, finite element numerical simulation has been performed to obtain the mechanical response, i.e., load-displacement curve, of the traditional Sn63-Pb37 eutectic solder alloy during the indentation process. A well-known visco-plastic constitutive model and the corresponding parameters [12–14] have been predefined to describe the mechanical behavior of Sn63-Pb37 solder. It is clearly showed that the obtained indentation load-displacement curves are significantly rate-dependent. Meanwhile, a physical analysis method based upon the concept of "work-of-indentation" has been proposed in order to derive the creep property

*Author to whom all correspondence should be addressed.
‡*Present address*: Yik Shing Tat Industrial Co., Ltd., Qianjin second Rd, 75 Zone (Beside Liutang Park), 76 Section, Xixiang, Bao'an District, Shenzhen, 518101, People's Republic of China.

of solder alloy, e.g., rate sensitivity, directly from the rate-dependent indentation load-displacement curves. The validity of the proposed method has been demonstrated by the good agreement between the derived and predefined value. Furthermore, such analysis method is applied for a Pb-free solder alloy to derive its rate sensitivity from the experimentally obtained indentation load-displacement curves. The derived value is consistent with the reported value for the same Pb-free solder alloy.

2. Finite element simulation of indentation process

The sharp indentation using Berkovich indenter, which is popular for indentation of soft material, has been simulated here. The indented material is the traditional Sn63-Pb37 eutectic solder alloy since its rate-dependent mechanical property is well known.

2.1. Finite element modeling

Fig. 1 shows the two-dimensional finite element model used in this work, only 1/2 of the indentation half-space was modeled due to the axial symmetry. The triangle pyramid Berkovich indenter was modeled as a conical body using a rigid line. The half-included angle θ of this conical indenter was set as 70.3° since it will give the same ratio of h/A as the Berkovich indenter which has $\theta = 65.3°$, where h is the penetration depth and A is the projected contact area. To avoid any far-field boundary effect, the total width and height of the mesh had to be at least 30 times the radius of the projected contact area. The generating mesh gradually increased the element sizes in the volume away from the center of contact in order to keep a balance between simulation accuracy and calculation time. As the boundary condition, all nodes at the bottom of the model are prevented from moving in the x and y directions; nodes along the symmetric axis are constrained in the x direction. Furthermore, a friction coefficient of 0.1 was introduced to consider the sliding between the indenter and the indented surface. The commercial finite element program ABAQUS® was used for this simulation and the model totally consisted of 3761 four-node axisymmetric elements with reduced integration.

In this study, the indenter was assumed to be rigid. The solder alloy was elastic-viscoplastic with creep and plastic deformation considered together. The creep strain rate is defined by the typical sine hyperbolic equation:

$$\dot{\varepsilon} = A(\sinh B\sigma)^{\mathrm{n}} \exp\left(\frac{-\Delta H}{RT}\right) \tag{1}$$

where $\dot{\varepsilon}$ is the uniaxial equivalent creep strain rate, σ is the equivalent stress, ΔH is the activation energy, R is the universal gas constant, T is the temperature in Kelvin, n is the creep stress sensitivity, A and B are material constants. The material properties of Sn63-Pb37 solder were obtained from [15] and listed in Table I.

It has been known that the microstructure of the indented Sn63-Pb37 alloy is heterogeneous, therefore, a large maximum indentation load of 500 mN was selected for the simulation in order to obtain the global mechanical response for the heterogeneous material, but not for individual phase. The indentation process was simulated by load-control, at constant loading speeds of 0.25, 1, 5, 10, 20,50, 100 and 200 mN/s. To examine the indentation creep behavior, the maximum load was kept constant for 5 s before unloading. The test temperature was set to be 298 K.

2.2. Simulation results

Fig. 2 shows a typical indentation load-displacement curve obtained from the above simulations. The indentation load, which increases at a constant loading rate, leads to a nonlinearly increase of the penetration depth. After the load reaches the given maximum value of P_{m}, a creep penetration occurs during the hold time and the depth increases from h_{ml} (depth at the end of loading) to h_{mu} (depth at the beginning of unloading). Finally, the penetration depth decreases during the unloading process until the load approaches zero and a residual depth h_{r} is left.

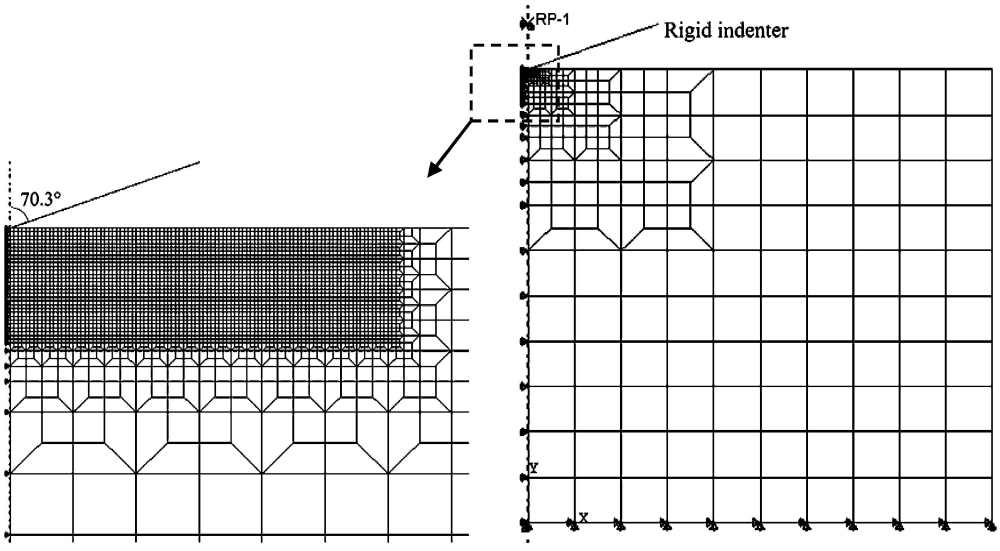

Figure 1 The Axisymmetric finite element mesh and boundary conditions showing successively finer elements in the vicinity of the indenter.

TABLE I Sn-Pb eutectic solder properties used in FE model ($T = 298$ K)

Elastic properties		Plastic properties				
Young's modulus (MPa)	Poisson's ratio	Yield stress (MPa)	Plastic strain	Yield stress (MPa)	Plastic strain	Creep properties
30425	0.3	13.8	0	96.5	7.93E-01	Equation 1:
		27.6	7.30E-04	110	1.67E + 00	$A = 1127.79$ 1/K
		41.4	7.02E-03	124	3.22E + 00	$B = 64140.95\ \mu m^2/N$
		55.2	3.49E-02	138	5.80E + 00	$n = 3.3$
		68.9	1.21E-01			$\Delta H = 52890$ J/Kg
		82.7	3.36E-01			$R = 8.314$ J/(Kg·K)

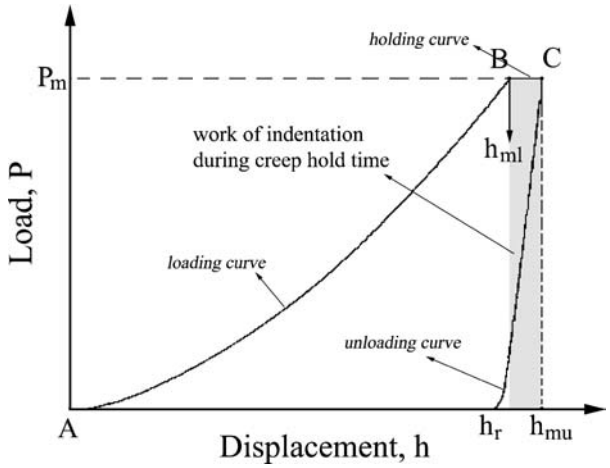

Figure 2 Typical indentation load-displacement curve for rate-dependent creep solder alloys.

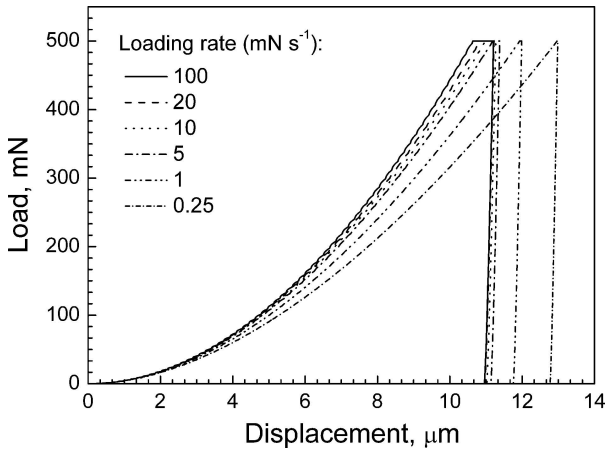

Figure 3 Load-displacement indentation curves with changing the loading rate for Sn-37Pb solder alloy from FE model.

Fig. 3 shows the indentation load-displacement curves of the indented Sn63-Pb37 solder obtained from the simulation results with different loading rates. Fig. 4 shows the rate-dependent characteristics of penetration depth. First, although the maximum indentation load is the same, a slower loading rate leads to a deeper penetration depth h_{ml}, i.e., lower indentation hardness and yield stress. Second, during the same hold time, a higher loading rate leads to a larger creep penetration Δh, which indicates a resulting higher creep strain rate.

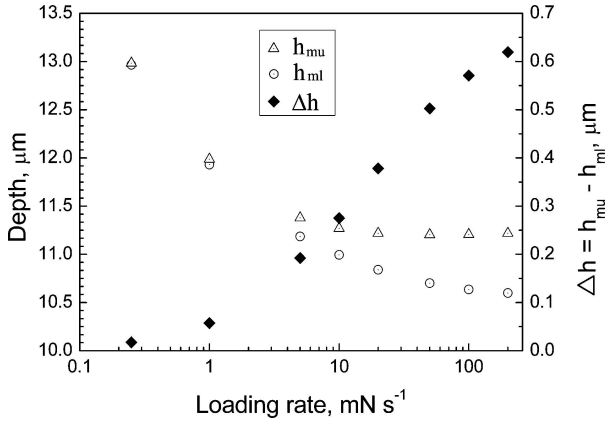

Figure 4 Rate-dependent penetration depth of Sn-37Pb solder alloy from FE model.

3. Physical analysis of rate-dependent indentation load-displacement curves

Several physical analysis methods have been illustrated to be effective to derive the elastic and rate-independent plastic properties from the indentation load-displacement curves [8, 16, 17].

For these load-displacement curves, the elastic modulus of indented material could be measured with Oliver-Pharr method [16]; the plastic properties, e.g., yield stress, of tested material could be determined from methods proposed in Giannakopoulos's papers [8, 17]. However, there are no credible methods for the derivation of rate-dependent properties from the indentation curves. In this paper, it could be expected to determine the creep properties, i.e. rate sensitivity (n) of the indented material from the holding step in rate-dependent indentation curves.

According to Equation 1, at the uniform temperature of 298 K, the relation between creep strain rate and creep stress may be expressed in another way:

$$\dot{\varepsilon} \propto (\sinh B\sigma)^{n} \quad \text{or} \quad \ln \dot{\varepsilon} \propto n \ln(\sinh B\sigma) \qquad (2)$$

The value of n is usually named as creep stress sensitivity related with creep strain rate and can be derived from the σ versus $\dot{\varepsilon}$ curve of conventional creep tests. Since it is very difficult to directly determine the stress and strain rate during an indentation test, certain measures with a reasonable physical definition, with values that can be directly calculated from the indentation load-displacement curve, are suggested in this work.

Here we consider the definition of indentation hardness proposed by Stilwell and Tabor [18]. They

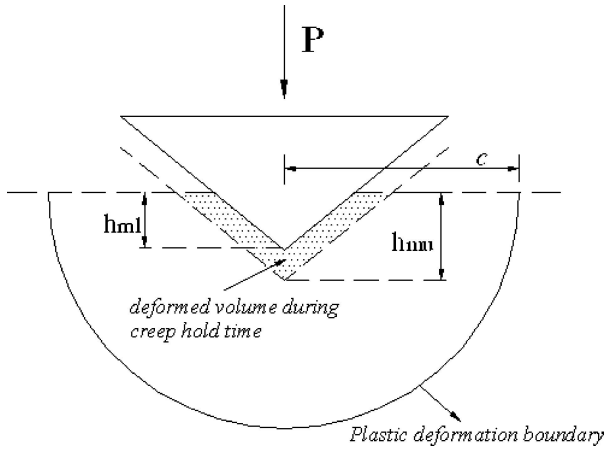

Figure 5 Schematic of creep deformed volume during hold time in an indentation test.

proposed the concept of "work of indentation" and suggested that indentation hardness could be defined as:

$$H = \frac{W_P}{V_P} \tag{3}$$

where W_P is the plastic work done during the indentation process, V_P is the plastically deformed volume in the indented material. The physical meaning of Equation 3 is that, indentation hardness, which reflects the deformation extent of the indented materials, can be understood as the energy expenditure per unit volume during indentation [18, 19]. Following this idea, for the indentation process of rate-dependent material, after the loading stage (line AB in Fig. 2) that leads to inelastic deformation in the indented material, all of the work-of-indentation W_{cr} during the hold time (the shadow area in Fig. 2) can be considered to contribute to the irreversible increase of the creep deformed volume V_{cr}. Therefore, we can define the indentation hardness of creep material H_{cr} as:

$$H_{cr} = \frac{W_{cr}}{\Delta V_{cr}} \tag{4}$$

As illustrated in Figs. 3 and 5, W_{cr} and V_{cr} can be calculated as:

$$W_{cr} = P_m(h_{mu} - h_{ml}) \tag{5}$$

$$\Delta V_{cr} = \frac{g}{3}\left(h_{mu}^3 - h_{ml}^3\right) \tag{6}$$

where g is a geometric factor and is equal to 24.56 for the Berkovich indenter, i.e., the projected contact area of the Berkovich indenter is 24.56 h^2.

Also, as shown in Fig. 5, there exists a hemispherically shaped elastoplastic boundary, which separates the plastically deformed volume surrounding the sharp penetration. The so-called "cavity" model of Johnson [20] can be applied to extract the hemi-spherically shaped elastoplastic boundary as follows:

$$c = \left[\frac{3P_m}{2\pi\sigma_y}\right]^{1/2} \tag{7}$$

where σ_y is the uniaxial yield strength. The relationship between hardness and uniaxial stress is often estimated by

$$H = C\sigma_y \tag{8}$$

where C is constant and is between 2.7–3.3. In this paper C was set as 2.8, as the value provided from Tabor [21] and Mata *el al.* [22]. As the effective Mises stress contour shown in Fig. 6, from the 2D FE model with the loading rate of 50 mN·s^{-1} after the loading step for Sn-37Pb eutectic solder, the elastoplasitc boundary is really hemi-spherically shaped, as the dotted line in Fig. 6, and its plastic zone radius c is about 62 μm according to Equation 7 for indentation model. Furthermore, the change of plastic zone radius during holding step in FE simulation is lower than 5 μm. Therefore, we assume that for creep indentation during the hold time, plastically deformed volume V_P of the indented material remains invariable due to the smaller change of plastic zone radius and the constant values of the indentation load and creep indentation hardness defined by Equation 4. Thus, the corresponding creep strain rate can be related to the volumetric creep strain occurring during the hold time, which is the ratio of change in deformed volumes ΔV_{cr} to the normalization volumes given by V_P:

$$\dot{\varepsilon}_{cr} = \frac{\Delta V_{cr}}{V_P}\frac{1}{\Delta t} = \frac{3\Delta V_{cr}}{\pi c^3}\frac{1}{\Delta t} \tag{9}$$

where Δt is the hold time for creep indentation and is equal to 5 s in this FE models.

According to the above analysis, creep stress sensitivity of the Sn-Pb eutectic solder can be determined from the $\ln(\sinh B\sigma)$ vs $\ln\dot{\varepsilon}_{cr}$ curve, represented by Equation 2, where both magnitudes can be directly calculated from the indentation load versus depth curve. Fig. 7 shows the calculation results. It can be seen that the derived result gives almost the same value of stress sensitivity predefined in the FE model. Therefore, by means of the creep indentation tests with different loading rates, the above physical analysis will be applicable to the lead-free solder alloy.

4. Application to experimental results on lead-free solder

Sn-3.5Ag-0.75Cu alloy, which was recommended as the best candidate of lead-free solders [23], was used in this work. Microindentation tests were performed at room temperature by using Micro Zone Tester (Akashi Co., Japan) with a Berkovich indenter. The specimen with 20 × 20 × 12 mm volume was chemically polished to remove the surface layer before the test. A large maximum load of 500 mN was selected for the microindentation in order to obtain the global mechanical response for the heterogeneous material, but not for individual phase. The indentation was carried out by load-control, at constant loading speeds of 0.25, 0.5, 1, 2, 5, 10, 20, 50 and 100 mN·s^{-1}. The maximum load was kept constant for 5 seconds before unloading, and

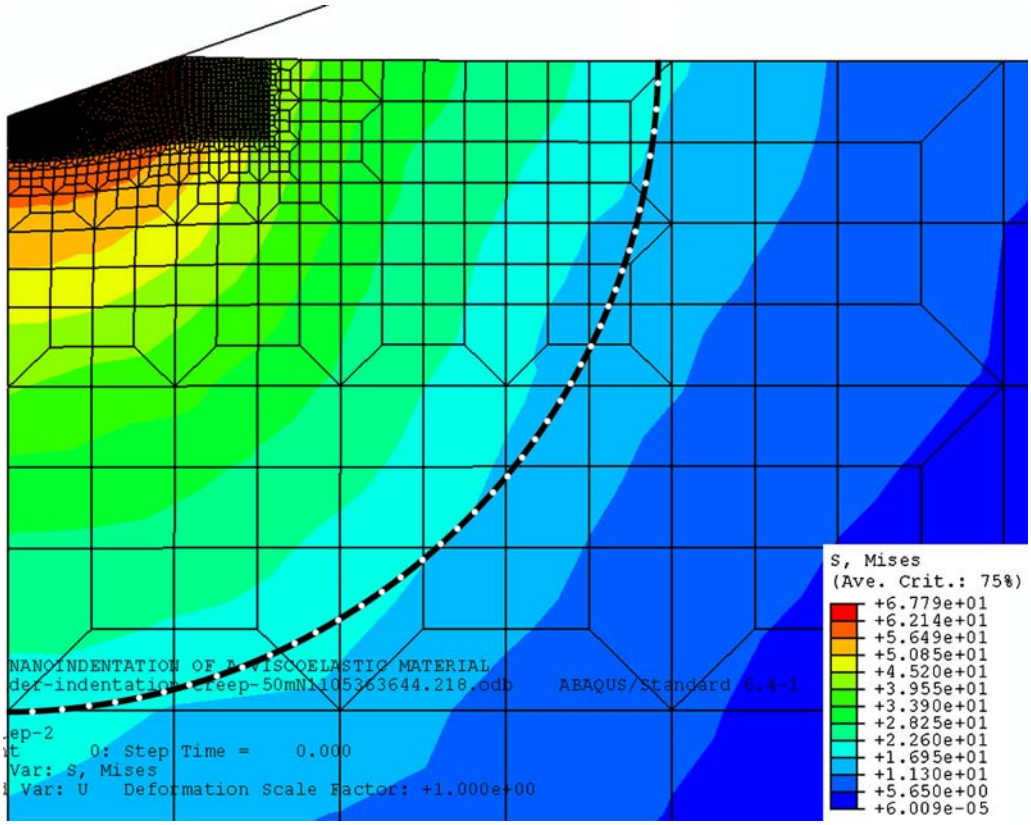

Figure 6 Mises stress contour for Sn-37Pb solder alloy from FE model with loading rate of 50 mN·s^{-1}.

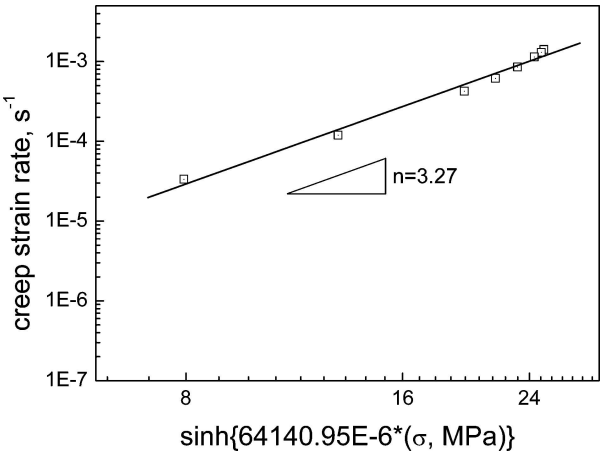

Figure 7 Derived values of creep stress sensitivity for the Sn-37Pb eutectic solder alloy from FE simulations.

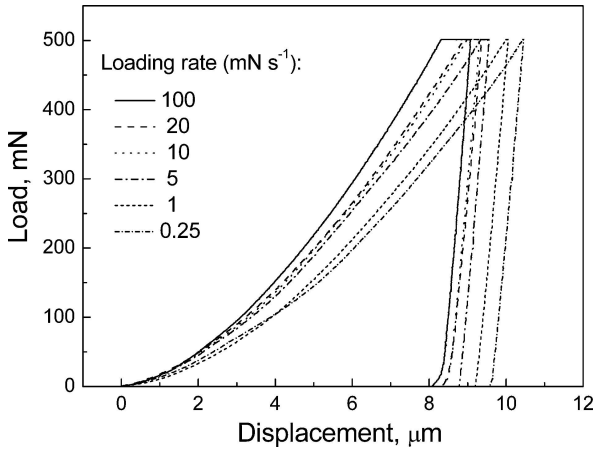

Figure 8 Load-displacement indentation curves with changing the loading rate for Sn-3.5Ag-0.75Cu solder alloy.

then the unloading rate was 500 mN·s^{-1}. Fig. 8 shows some typical load-displacement curves with different loading rate in indentation experiments.

Due to the unknown constant B in Equation 1, the solder creep law was given in another Norton Equation:

$$\dot{\varepsilon} = A\sigma^{n} \exp\left(-\frac{\Delta H}{RT}\right) \tag{10}$$

At the temperature of 298 K, Equation 10 can be given as

$$\dot{\varepsilon} \propto \sigma^{n} \quad \text{or} \quad \ln \dot{\varepsilon} \propto n \ln \sigma \tag{11}$$

The physical analysis given in Section II can be used to derive the creep stress sensitivity, n. Fig. 9 shows

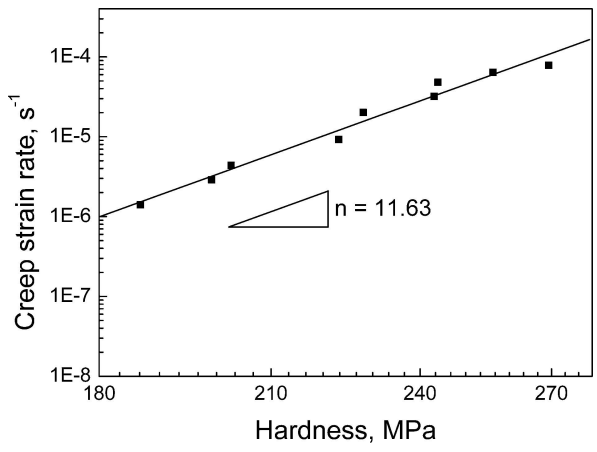

Figure 9 Derived values of creep stress sensitivity for the Sn-3.5Ag-0.75Cu solder alloy.

the derived result for the Sn-3.5Ag-0.75Cu solder alloy used in this work. The result of creep stress sensitivity ($n = 11.63$) from indentation tests can be comparable to that from the tensile creep tests for Sn-Ag-Cu ($n = 12.0$) given by Wiese *et al.* [24].

5. Conclusions

(1) Finite element simulations of visco-plastic indentation in a typical creep material, Sn-37Pb eutectic solder alloy, are performed with different loading rates by a rigid conical indenter (70.3° half-included angle). The results show that the indentation load-displacement curves are loading-rate-dependent. A slower loading rate leads to a deeper penetration depth in loading step, instead a smaller creep depth in holding step.

(2) The concept of "work of indentation" is introduced for the definition of creep indentation hardness and creep yield stress. The volume strain occurring during the creep hold time is measured for the definition of creep strain rate. Thus creep stress sensitivity can be determined from the relationship between the creep stress and creep strain rate. The derived value of n is consistent with the predefined value.

(3) The above physical process is used to analyze the load-displacement curves from the Berkovich indentation of Sn-3.5Ag-0.75Cu lead-free solder. Such methods provide not only a cost and time-saving method, but also a possible manner to obtain the material parameters form a small volume in the dimension of micrometer, if combined with other researchers' results about the determination of the elastic and plastic properties from indentation curves.

References

1. J. GLAZER, *Intern. Mater. Rev.* **40** (1995) 65.
2. M. ABTEW and G. SELVADURAY, *Mater. Sci. Eng. Reports* **27** (2000) 95.
3. K. SUGANUMA, *Curr. Opin. Solid State Mater. Sci.* **5** (2001) 55.
4. M. FUJIWARA and M. OTSUKA, *Mater. Sci. Eng. A* **319–321** (2001) 929.
5. C.-M. CHENG and Y.-T. CHENG, *Appl. Phys. Lett.* **71** (1997) 2623.
6. A. E. GIANNAKOPOULOS and S. SURESH, *Scripta Mater.* **40** (1999) 1191.
7. M. SAKAI, *J. Mater. Res.* **14** (1999) 3630.
8. K. ZENG and C.-H. CHIU, *Acta Mater.* **49** (2001) 3539.
9. P.-L. LARSSON, *Int. J. Mech. Sci.* **43** (2001) 895.
10. J. H. LAU (eds.), "Solder Joint Reliability: Theory and Application" (Von Nostrand Reinhold, New York, 1992).
11. W. J. PLUMBRIDGE, *J. Mater. Sci.* **31** (1996) 2501.
12. R. DARVEAUX and K. BANERJI, *IEEE Trans. CHMT.* **15** (1992) 1013.
13. X.-Q. SHI, Z.-P. WANG, *et al.*, *ASME J. Electron. Packag.* **124** (2002) 85.
14. Y. WEI, C.-L. CHOW, H.-E. FANG and M.-K. NEILSEN, *ibid.* **123** (2001) 278.
15. A. DESHPANDE, G. SUBBARAYAN and D. ROSE, *ibid.* **122** (2002) 6.
16. W. C. OLIVER and G. M. PHARR, *J. Mater. Res.* **7** (1992) 1564.
17. T.-A. VENKATESH, K.-J. VAN VLIET, A.-E. GIANNAKOPOULOS and S. SURESH, *Scripta Mater.* **42** (2000) 833.
18. N.-A. STILWELL and D. TABOR, *Proc. Phys. Soc.* **78** (1961) 169.
19. J.-R. TUCK, A.-M. KORSUNSKY, S. J. BULL and R. I. DAVIDSON, *Surf. Coat. Technol.* **137** (2001) 217.
20. K.-L. JOHNSON, *J. Mech. Phys. Solids* **18** (1970) 115.
21. D. TABOR, "Hardness of Metals," (Oxford University Press, London, 1951).
22. M. MATA, M. ANGLADA and J. ALCALÁ, *J. Mater. Res.* **17** (2002) 964.
23. B. P. RICHARDS *et al.*, "An Analysis of the Current Status of Lsead-free Soldering," NPL and ITRI Report (1999).
24. S. WIESE, E. MEUSEL and K.-J. WOLTER, 53rd ECTC 2003, p. 197.

Received 27 September
and accepted 15 November 2004